Biological particle manipulation: an example of Jurkat enrichment

Emre Altinagac[1], *Huseyin Kizil*[1,2], *Levent Trabzon*[1,3]

[1]*Department of Nanoscience & Nanoengineering, Istanbul Technical University, Istanbul 34396, Turkey*
[2]*Department of Metallurgical and Materials Engineering, Istanbul Technical University, Istanbul, Turkey*
[3]*Department of Mechanical Engineering, Istanbul Technical University, Istanbul, Turkey*
E-mail: altinagac@itu.edu.tr

Published in Micro & Nano Letters; Received on 11th May 2015; Accepted on 30th July 2015

Dielectrophoresis-based separation of microparticles and living cells are studied with computational and experimental methods. The flow behaviours of particles are modelled and simulated using COMSOL Multiphysics 4.3a software (COMSOL Ltd). Lab-on-a-chip devices having a titanium (Ti) interdigitated electrode layer on a glass substrate and a PDMS microchannel are fabricated to investigate the most effective design for separating particles based on their sizes. Polystyrene particles in different diameters (3.2 and 9.8 μm) are used in the experiments. Green polystyrene particles from red ones are fully separated in a current design. Enrichment of Jurkat cells having 10.1 average diameter in phosphate buffer solution (PBS) medium is achieved.

1. Introduction: There is a growing interest in understanding the cellular behaviour or biochemical analysis of cells in medicine and bio-technology applications [1–3]. Cells of different types have characteristic properties that make the enrichment, sorting or isolation of cells possible in a microfluidic platform [4–7]. Isolation of individual cells from complex mixtures is crucial in case of discriminative analysis of target cells. There is a great demand for a rapid and high-performance cell sorting with a portable and cost effective design that can be used for point of care applications. 'Lab-on-a-chip (LOCs) devices' create inexpensive and efficient solutions by integrating several laboratory functions on a single chip of only a few centimetres in size [8–10]. LOCs are used in biomedical and environmental applications such as fluid transport, drug delivery, diagnosis of viruses and bacteria and manipulation of particles for focusing and separation applications.

Microfluidic cell sorting methods can be grouped mainly as 'fluorescence activated based', bead-based and label free cell sorting systems [11]. Label free cell sorting methods are attractive for having no effect on viability, size, shape, density, elasticity and polarisability of cells which means that the separation force is only dependent on differences in intrinsic physical properties of cells. Cells are sorted or isolated in label free passive, no external force applied, sorting systems by inertial forces, hydrodynamic spreading, deterministic lateral displacement and filtration which may require high flow rates, more than 2000 μl/min to reach desired efficiency and higher flow rates lead to higher physical damage on cells, which decrease the viability. In flow rates that the cell viability is stable, active sorting systems such as acoustophoresis and magnetophoresis can be adopted but the electrokinetic sorting systems have a wider range of cell types that can be applied to.

'Dielectrophoresis (DEP)' method is based on a force acting on a dielectric particle when it is subjected to a non-uniform electric field of either DC or AC field. A dielectric particle polarises under a non-uniform electric field and there is a net dipole moment acting on it. Each type of cells has a unique polarisability, size and viability, which makes the method useful for a target cell manipulation. The dominant dielectrophoretic force on a particle can be created with a planar microelectrode array, which is one of the best option for disposable point of care applications as they are inexpensive and requires no complex fabrication steps among other DEP-based designs.

2. Theory and design of experiments: Particles interact with non-uniform electric fields in two ways. Particles are trapped in intense electric field regions under 'positive DEP'. While they are pushed away from the regions under 'negative DEP (nDEP)'. The electrical properties of the particles and the frequency of the applied electric field determine the behaviour of DEP. The time averaged dielectrophoretic force on the particle is given by [12]

$$F_{\mathrm{DEP}} = 2\pi\varepsilon_0\varepsilon_m a^3 Re\left(f_{\mathrm{CM}}\right)\nabla E^2 \tag{1}$$

$$Re\left(f_{\mathrm{CM}}\right) = \left(\varepsilon_p^* - \varepsilon_m^*\right)/\left(\varepsilon_p^* + 2\varepsilon_m^*\right) \tag{2}$$

where ∇E^2 in (1) is the gradient of the root mean square of the electric field, f_{CM} is the 'Clausius–Mossotti (CM) factor' which is a function of particle and fluid properties, determines the direction of the dielectrophoretic force and $\mathrm{Re}(f_{\mathrm{CM}})$ indicates the real part of CM factor, and ? is the diameter of the particle [12].

Primarily, polystyrene particle separation based on their diameters in DI water is studied both theoretically and experimentally to come up with a proper design that is also applicable to biological cells. CM factor is calculated using (2) and can be seen in Fig. 1. ε^* in (2) is the complex permittivity of particle and medium and it is dependent on the applied frequency. The frequency of 2 MHz is applied during the experiments as it is found that the nDEP is effective in this region. Microfluidic channel with interdigitated electrodes on the bottom is seen in Fig. 2. The height of the microchannel is restricted to 20 μm so as to keep the particles in a region where DEP is still effective since the nDEP also pushes the particles along the z-axis and the electric field gradients are weakened over a short distance. The width of the microchannel is 500 μm and the interdigitated microelectrodes are placed at 45° angle on the bottom surface. The thickness of the Ti microelectrodes is 200 nm and the width and separation between the electrodes are 50 μm.

Numerical simulation of polystyrene particle trajectories is also carried out before the experiments with COMSOL 4.3a. The geometry and the boundary conditions are adapted to the design [13, 14]. Particles are pushed away perpendicularly from the interdigitated electrodes and with the addition of hydrodynamic drag force on the system the direction of total force on particles is along the microelectrode geometries. The total force acts on particles is schematically represented in Fig. 3.

We have studied the separation of different sized polystyrene particles (3.2 and 9.8 μm) and the most effective separation regarding our design is achievable within a flow rate of 1–10 μl/min when the applied potential is $10_{\mathrm{p-p}}$ at 2 MHz. Particle trajectories in the

doi: 10.1049/mnl.2015.0185

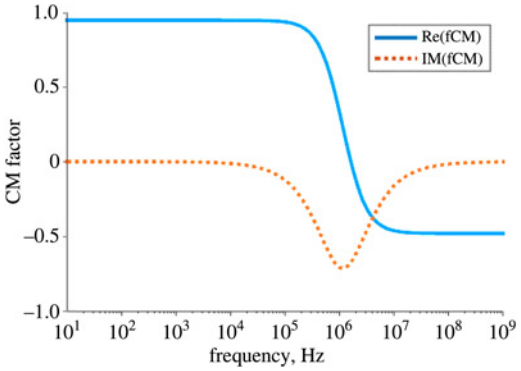

Fig. 1 *Numerically calculated CM factor for polystyrene particles in DI water*

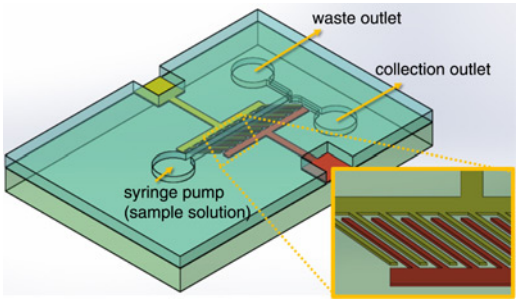

Fig. 2 *Schematic representation of designed microsystem for enrichment of biological particles*

microchannel are given in Fig. 4*a*. The particles with a diameter of 9.8 µm are deflected along the microelectrodes where the particles that are 3.2 µm are not affected by DEP because of the dominant hydrodynamic drag force. If the flow rate is kept below 1 µl/min, small particles are also influenced by DEP and separation is not occurred. Identically, increasing the flow rate also prevents separation since there is not enough dielectrophoretic force to counter the drag force. Average DEP force and particle positions depending on the particle diameter along time are given in Figs. 4*b* and *c*. The numerical results correlate with the theory.

3. Materials and methods: LOCs with a Ti interdigitated electrode layer on a glass substrate and a PDMS microchannel is fabricated to investigate the most effective design for separating particles based on their sizes. The standard photolithography techniques and lift-off processes are used. Thickness of the Ti electrodes on

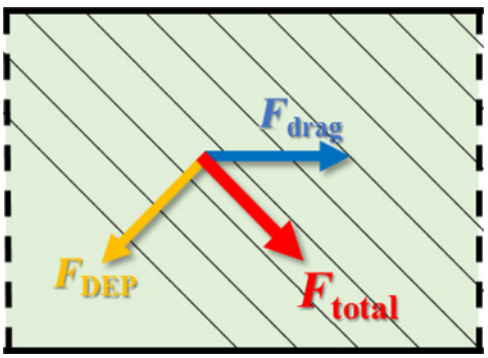

Fig. 3 *Schematic representation of the effective forces on the system (top view). Thin lines represent the interdigitated microelectrode geometries placed at 45° angle on the bottom of the microchannel*

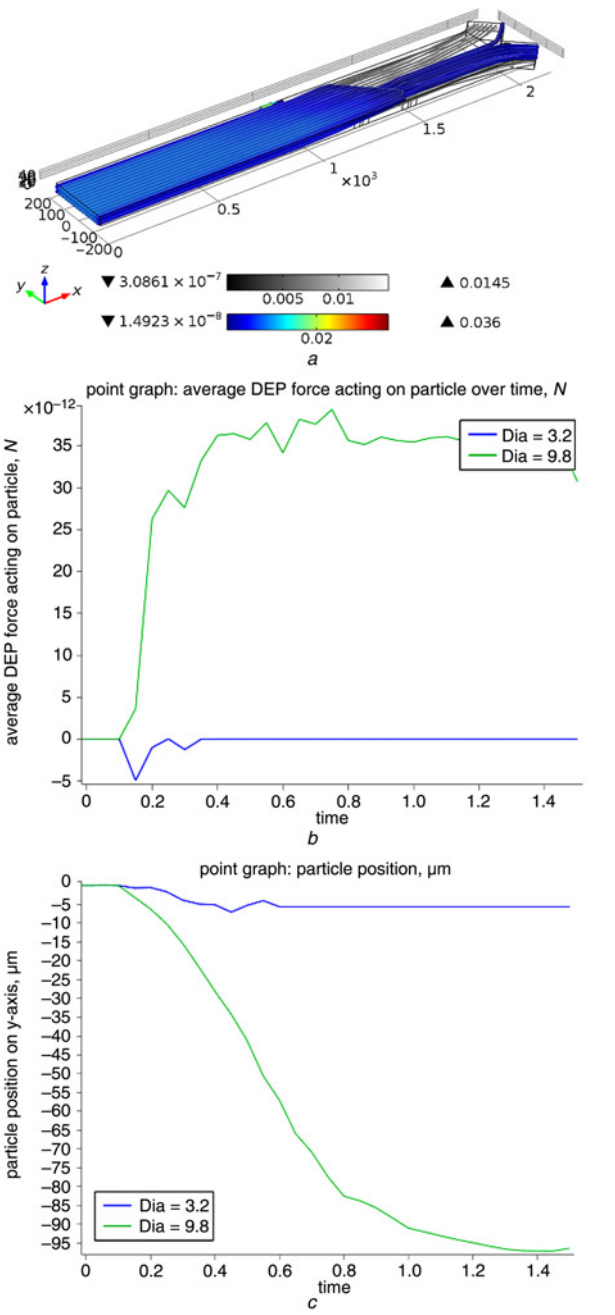

Fig. 4 *Numerical simulations are carried out with COMSOL 4.3a*
a Particle trajectories along the microchannel. Blue streamlines represent the 9.8 µm polystyrene particles and grey streamlines for 3.2 µm
b Average DEP force acting on the particles along time. About 9.8 µm particles are deflected along the microchannel due to the effective dielectrophoretic force acting on them
c Positions of particles on the *y*-axis along time is given. Without an effective dielectrophoretic force on 3.2 µm particles, there is no deflection on the *y*-axis

quartz glass bottom is 200 nm. The width and the gap between the electrodes is the same and 50 µm. Interdigitated electrodes are placed at 45° angle along 1 mm long microchannel. The width of the microchannel is 500 µm and the height is 20 µm. A signal generator, '81150A Pulse Function Arbitrary Noise Generator, Agilent Technologies (USA)' is connected to LOC and applied 10 V_{p-p} signal to connection wires using alligator clips shown in Fig. 5. Fluid flow is provided by two 'Harvard Pump 11 Plus Single Syringe Pump' for each inlet. About 100 µl Hamilton Syringes are used in syringe pump.

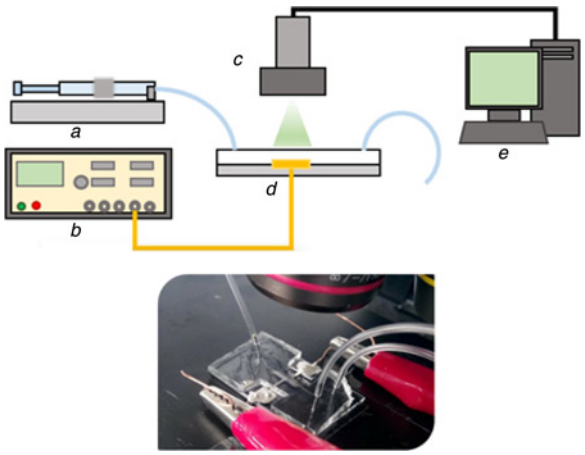

Fig. 5 *Schematic representation of experimental setup and a fabricated microfluidic chip*
a Syringe pump
b Signal generator
c Fluorescent optical microscope
d Fabricated LOC
e Computer

4. Experimental results and discussion: Particles are randomly distributed along the *y*-axis until they reach the electrodes since there is a single inlet. Along the electrode array, the particles with 3.2 µm in diameter (florescent red) are not affected by DEP since there is not enough force created on them due to their small diameters but the particles with 9.8 µm in diameter (florescent green) are deflected along the microchannel and collected only from one outlet. It is found that our simulations demonstrate well correlation with the experimental results. The efficient enrichment of particles based on their sizes is achieved with the current design and is convenient to be optimised by scaling the electrode geometries and microchannel height for various types of cells and particles. A microchannel with two inlets is designed to achieve 100% separation to prevent the distribution of particles at the beginning. The particles are focused on one side of the channel with a buffer inlet and the separation is achieved. The experimental result is given in Fig. 6. The flow rate is 7 µl/min and the applied signal is 10 V_{p-p} at 2 MHz. All the particles were mixed at the beginning of microchannel (Fig. 6*a*) and then the red and green particles were fully separated when they were exposed to DEP force in the system, as seen in Fig. 6*c*.

Single inlet microchannel design is used to separate Jurkat (T-lymphocytes) cells. The cells are labelled with a fluorescent marker (CFSE) for easier observation of the cell movement under a fluorescent optical microscope. Before the test, cells are pelletised

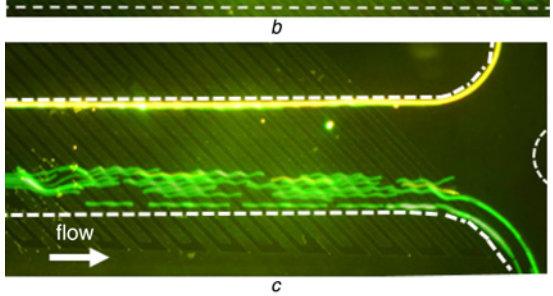

Fig. 6 *Separation of polystyrene particles in different diameters. Particles are focused on one side of the channel at the beginning with a buffer inlet*
a Particles are 9.8 µm (green) are deflected along the microelectrodes
b 3.2 µm (red) particles are collected from the waste outlet without any deflection
c White dash represents the microchannel sidewalls)

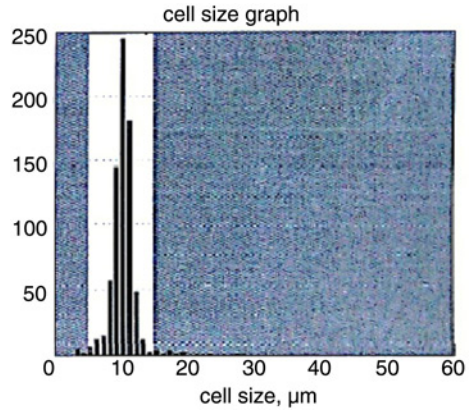

Fig. 7 *EVE Automatic Cell Counter results for Jurkat cells. Total cell concentration is 3.9 × 10^6 cells/ml and the viability is 93%*

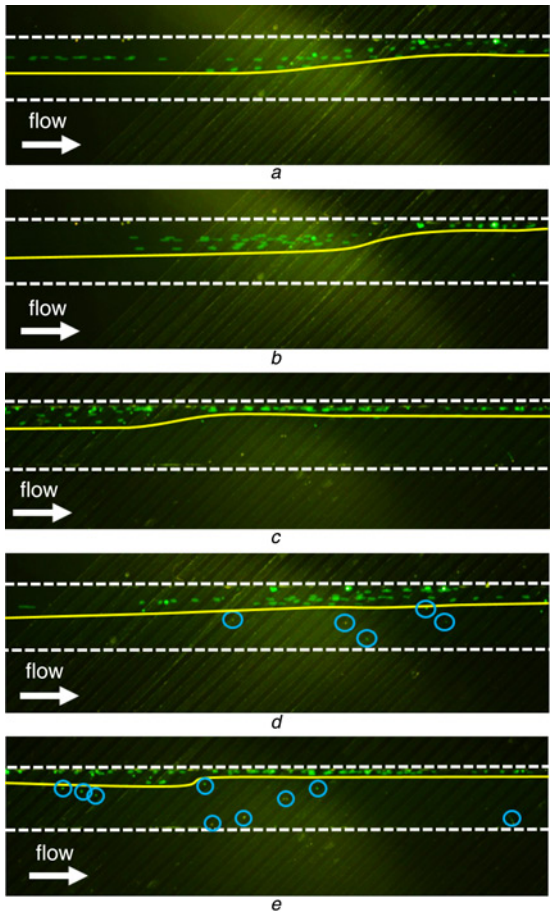

Fig. 8 *Experimental results for Jurkat cells. The enrichment of cells is expressed with yellow line and the microchannel sidewalls are expressed with white dash*
a–c Cells with larger diameters are focused on one side of the microchannel along microelectrode geometry
d, e Cells with smaller diameter (expressed with blue circle) are not affected by a dominant dielectrophoretic force

doi: 10.1049/mnl.2015.0185

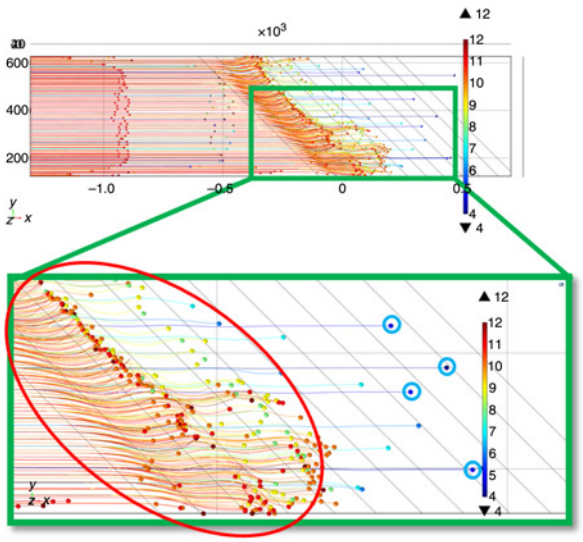

Fig. 9 *Trajectories for the particles with a characteristic size distribution of Jurkat cells. Particles with diameters >6 μm are deflected along the microelectrodes and curved trajectory of particles is expressed in red circle as the particles with diameters <6 μm are not affected by DEP and dragged linearly through the microchannel*

by centrifugation at 1000 rpm for 5 min and supernatant is discarded. About 0.8 μl CFSE is applied for 10×10^6 cells and cell pellet is dissolved in diluted CFSE. Dissolved cells are incubated at room temperature for 5 min. After washing the cells two times with 5 ml 5% FBS+PBS solution as blocking dye, cell pellet is dissolved in PBS.

The diameter of Jurkat cells is measured with EVE Automatic Cell Counter and the average diameter is 10.1 μm as can be seen in Fig. 7. The experimental results for Jurkat cells are given in Figs. 8 and 9. nDEP is effective in PBS medium under applied signal which is 10 V_{p-p} at 550 kHz. The deflection on the *y*-axis becomes clear below the flow rates of 3 μl/min. As in the case of polystyrene particles, Jurkat cells with larger diameters are deflected on the *y*-axis along the microelectrode geometry and given in Figs 8*a* and *b*. It is experimentally observed that near the end of microchannel cells with larger diameters are completely focused on one side of the microchannel as in Fig. 8*c*. The cells with smaller diameters are not affected by a dominant dielectrophoretic force and leave the channel without any deflection. Distribution of small cells are expressed with blue circles for each individual cells in Figs. 8*d* and *e*. The enrichment of Jurkat cells based on their diameter is achieved with the current design.

As a case scenario, we took the size distribution of Jurkat cells and adopted it in our numerical simulations excluding the electrical properties of each individual cell as the thickness of each layer in cell structures such as cytoplasm and membrane leading to individual complex permittivity for each cell. Our simulation results correlate with the experimental results and trajectories for polystyrene particles in DI water with a characteristic size distribution of Jurkat cells can be seen in Fig. 8. Applied flow rate is 2 μl/min and the signal is 10 V_{p-p}. The particles with a diameter lower than 6 μm are not affected by dielectrophoretic force as the particles with larger diameters are clearly deflected along the microelectrode geometry. According to results in Fig. 8, it can be claimed that size-dependent enrichment of cells or particles can be achieved.

5. Conclusions: We have studied the separation of different sized polystyrene particles (3.2 and 9.8 μm) and the most effective separation regarding our design is achievable within a flow rate of 1–10 μl/min when the applied potential is 10_{p-p} at 2 MHz. A microchannel with two inlets is designed to achieve 100% separation to prevent the distribution of particles at the beginning. The particles are focused on one side of the channel with a buffer inlet and the separation is achieved. Our simulations demonstrate a correlation with the experimental results. The efficient separation of particles by DEP based on their sizes and enrichment of Jurkat cells are achieved. nDEP is effective in PBS medium under applied signal which is 10 V_{p-p} at 550 kHz. The deflection on the *y*-axis becomes clear below the flow rates of 3 μl/min. Current channel design could be optimised by scaling the electrode geometries and microchannel height and used for separation of various types of cells or size-dependent enrichment of a homogenous culture or particles.

6. Acknowledgments: The authors acknowledge the financial support provided by the Scientific and Technological Research Council of Turkey (TUBITAK) under grant no. 111M730. The authors thank A.S. Yazgan and R. Fucucuoglu who provided insight and expertise that greatly assisted the research. And Z.S. Yunt for her support for the measurement of cell diameters.

7. References

[1] Kraus J.D.: 'The square-corner reflector'. European Microwave Conf., Rome, Italy, 2011, pp. 19–24
[2] Wait J.R.: 'On the theory of an antenna with an infinite corner reflector', *Can. J. Phys.*, 2009, **32**, (6), pp. 365–371
[3] Olver A.D., Sterr U.O.: 'Study of corner reflector antenna using FDTD'. Proc. Int. Conf. on Antennas and Propagation, Edinburgh, UK, April 1997, vol. 1, pp. 334–337
[4] Taflove A.: 'Computational electrodynamics' (Artech House, Norwood, MA, 1995)
[5] Wait J.R.: 'Theory of an antenna with square-corner reflector', *Can. J. Phys.*, 1954, **23**, (4), pp. 215–222
[6] Kraus J.D.: 'The square-corner reflector'. Available at http://www.theiet.org, accessed 22nd November 2010
[7] Mateo J., Gerlinger M., Rodrigues D., de Bono J.S.: 'The promise of circulating tumor cell analysis in cancer management', *Genome Biol.*, 2014, **15**, (8), p. 448
[8] Karabacak N.M., Spuhler P.S., Fachin F., *ET AL.*: 'Microfluidic, marker-free isolation of circulating tumor cells from blood samples', *Nat. Protocols*, 2014, **9**, (3), pp. 694–710
[9] Alix-Panabières C., Pantel K.: 'Technologies for detection of circulating tumor cells: facts and vision', *Lab Chip*, 2014, **14**, (1), pp. 57–62
[10] Jin C., McFaul S.M., Duffy S.P., *ET AL.*: 'Technologies for label-free separation of circulating tumor cells: from historical foundations to recent developments', *Lab Chip*, 2014, **14**, (1), pp. 32–44
[11] Hajba L., Guttman A.: 'Circulating tumor-cell detection and capture using microfluidic devices', *TrAC Trends Anal. Chem.*, 2014, **59**, pp. 9–16
[12] Čemažar J., Miklavčič D., Kotnik T.: 'Microfluidic devices for manipulation, modification and characterization of biological cells in electric fields – a review', *Electron. Compon. Mater.*, 2013, **43**, (3), pp. 143–161
[13] Chen J., Li J., Sun Y.: 'Microfluidic approaches for cancer cell detection, characterization, and separation', *Lab Chip*, 2012, **12**, (10), pp. 1753–1767
[14] Ríos Á., Zougagh M., Avila M.: 'Miniaturization through lab-on-a-chip: Utopia or reality for routine laboratories? A review', *Anal. Chim. Acta*, 2012, **740**, pp. 1–11
[15] Neuži P., Giselbrecht S., Länge K., Huang T.J., Manz A. : 'Revisiting lab-on-a-chip technology for drug discovery', *Nat. Rev. Drug Discov.*, 2012, **11**, (8), pp. 620–632
[16] Trietsch S.J., Hankemeier T., Van der Linden H.J.: 'Lab-on-a-chip technologies for massive parallel data generation in the life sciences: a review', *Chemometr. Intell. Lab. Syst.*, 2011, **108**, (1), pp. 64–75
[17] Shields IV C.W., Reyes C.D., López G.P.: 'Microfluidic cell sorting: a review of the advances in the separation of cells from debulking to rare cell isolation', *Lab Chip*, 2015
[18] Hoyoung Y., Kim K., Lee W.G.: 'Cell manipulation in microfluidics', *Biofabrication*, 2013, **5.2**, p. 022001
[19] Altinagac E., Genc Y., Kizil H., Trabzon L., Beskok A.: 'Continuous separation of polystyrene particles with AC dielectrophoresis based on their sizes'. Micromechanics and Microsystems Europe Workshop, Istanbul, Turkey, 2014
[20] Altinagac E., Genc Y., Kizil H., Trabzon L., Beskok A.: 'Microdevices for continuous sized based sorting by AC dielectrophoresis'. Fourth Micro and Nano Flows Conf., UCL, London, 2014